PREPARED FOR THE U.S. DEPARTMENT OF ENERGY,
UNDER CONTRACT DE-AC02-76CH03073

PPPL-3844
UC-70

PPPL-3844

Soft X-ray Tangential Imaging of the NSTX Core Plasma by Means of a MPGD Pin-hole Camera

by

D. Pacella, M. Leigheb, R. Bellazzini, A. Brez, M. Finkenthal,
D. Stutman, R. Kaita, and S.A. Sabbagh

July 2003

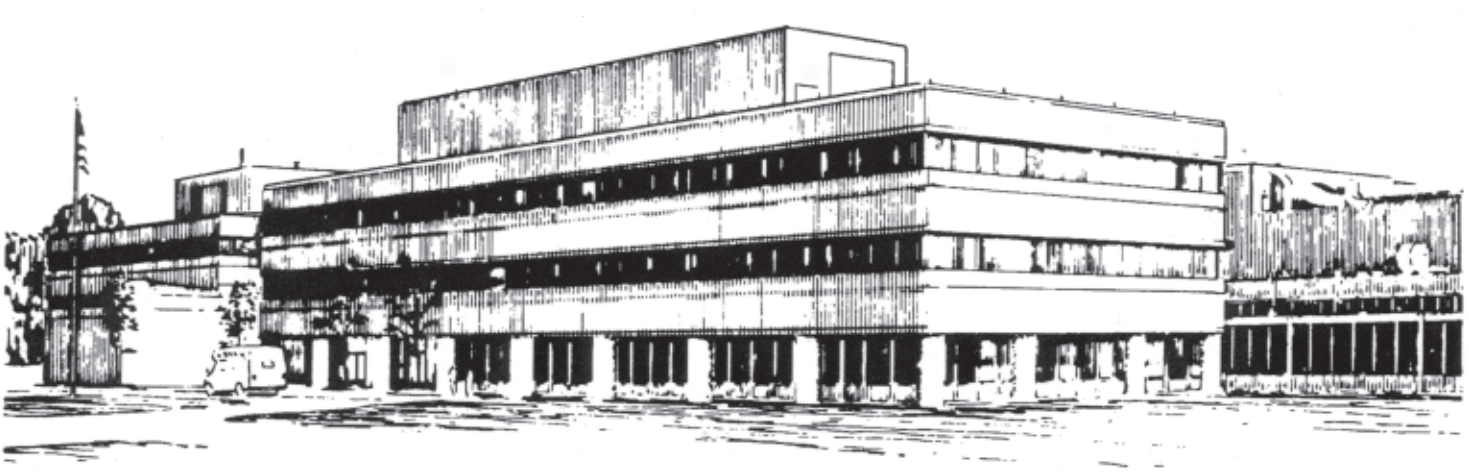

PRINCETON PLASMA PHYSICS LABORATORY
PRINCETON UNIVERSITY, PRINCETON, NEW JERSEY

PPPL Reports Disclaimer

Availability

This report is posted on the U.S. Department of Energy's Princeton Plasma Physics Laboratory Publications and Reports web site in Fiscal Year 2003. The home page for PPPL Reports and Publications is: http://www.pppl.gov/pub_report/

DOE and DOE Contractors can obtain copies of this report from:

U.S. Department of Energy
Office of Scientific and Technical Information
DOE Technical Information Services (DTIS)
P.O. Box 62
Oak Ridge, TN 37831

Telephone: (865) 576-8401

Fax: (865) 576-5728

Email: reports@adonis.osti.gov

This report is available to the general public from:

National Technical Information Service
U.S. Department of Commerce
5285 Port Royal Road
Springfield, VA 22161

Telephone: 1-800-553-6847 or
(703) 605-6000

Fax: (703) 321-8547

Internet: http://www.ntis.gov/ordering.htm

Soft-X ray Tangential Imaging of the NSTX core plasma by means of a MPGD pin-hole camera

D. Pacella[$], M. Leigheb[&], R. Bellazzini[*], A. Brez[*], M. Finkenthal[^], D. Stutman[#], R. Kaita[%], S.A. Sabbagh[£]

$ Present address: Plasma Spectroscopic Group, Johns Hopkins University, Baltimore, MD 21218
Permanent address: Associazione EURATOM-ENEA, CR Frascati, 00044 Frascati, Rome, Italy

& Associazione EURATOM-ENEA sulla Fusione, CR Frascati, 00044 Frascati, Rome, Italy

** INFN-Pisa and University of Pisa, Pisa Italy*

^ Present address: Plasma Spectroscopic Group, Johns Hopkins University, Baltimore, MD 21218
Permanent address: Racah Institute, Hebrew University, Jerusalem, Israel

Plasma Spectroscopic Group, Johns Hopkins University, Baltimore, MD 21218

% Princeton Plasma Physics Laboratory, Princeton, NJ, 08543

£ Department of Applied Physics and Applied Mathematics, Columbia University, New York City, NY)

ABSTRACT

A fast X-ray system based on a Micro Pattern Gas Detector has been used for the first time, to investigate emission from the plasma core of the National Spherical Tokamak eXperiment (NSTX), at the Princeton Plasma Physics Laboratory. The results presented in this work demonstrate the capability of such a device to measure with a time resolution of the order of 1 ms, the curvature and the elongation of the X-ray iso-emissivity contours, under various plasma conditions. Also, comparisons with the magnetic surface structure calculated by the EFIT code show good agreement between reconstructed flux surface and the soft-X ray emissions (SXR) for poloidal beta values up to 0.6. For greater values of beta, X-ray iso-emissivity contours become circular, while magnetic flux surface reconstructions yield elongation $1.5 < k < 2.2$

The X-ray images have been acquired with a (statistical) signal to noise ratio (SNR) per pixel of about 30. Thanks to the direct and efficient X-ray conversion and its operation in a photon counting mode, this new diagnostic tool allows the routine investigation of the plasma core with a sampling rate of 1kHz and extremely high SNR under all experimental conditions in NSTX.

INTRODUCTION

A new diagnostic system in the soft X ray range, for imaging of magnetic fusion plasmas, has been developed at ENEA Frascati (Italy) in collaboration with INFN-Pisa (Italy) [1, 2]. The device is a pinhole camera whose detector is a Micro Pattern Gas Detector (MPGD) [3,4] having a Gas Electron Multiplier (GEM) as its amplifying stage. A read-out board with 144 square pixels (2mm x 2mm) arranged in a 12 x 12 matrix pattern, has been designed for this purpose and coupled to a GEM foil with 2.5×2.5 cm active area. The electron signal, corresponding to the detected X ray photon, is collected at the pixel and processed by a fast charge pre-amplifier (LABEN 5231) and an amplifier (LABEN 5185). Discriminators and counters for all the channels form the data acquisition system, using the VME standard by CAEN. The fast, low noise electronics coupled to the discriminators and asynchronous scalers ensure high quality data resulting in only statistical noise, with single photon counting at high detection rates (up to 10^7 ph/s·pixel) and high framing rates (up to 100 kHz).

The spatial resolution and imaging properties of this detector have been proved [1] in conditions of high counting rates and high gain, with the detector fully illuminated by very intense X ray sources (laboratory tubes and tokamak plasma).

The system has been tested successfully at the Frascati Tokamak Upgrade (FTU) with a one-dimensional perpendicular view of the plasma, and then installed and used on National Spherical Tokamak Experiment (NSTX), where it had a full two-dimensional tangential view.

The gas mixture used for the MPGD is 80% Ne and 20% Dimethyl Ether (DME). The instrument has been set up in the experimental campaign described in this work for the photon energy range 3 – 8 keV; the detection efficiency of the whole system is quite flat for most of this interval [2].

The gain of each electronic amplifier connected to every pixel is adjusted in order to reproduce the same spectrum [2], with a precision of about 2%. Since each channel behaves as an independent spectrometer, it is necessary to perform these individual calibrations in order to exploit the

combination of imaging capability and energy discrimination, one of the most powerful features of the system. The energy resolution of the detector, in the mentioned energy range, is about 20%; therefore, the electronic discrimination of the pulse amplitude can be performed with this uncertainty.

EXPERIMENTAL SETUP ON NSTX

NSTX is a spherical tokamak [5] with major radius 85 cm, minor radius 70 cm, and a plasma volume of about 12 m^3. The shots considered in this work have a toroidal field on axis of 0.4 T, and maximum values of the central electron density and temperature of 8 10^{19} m^{-3} and 1.2 keV respectively.

The instrument has been set up on NSTX with a tangential view of the plasma. The pinhole (diameter 1 mm) is located close to the beryllium window of NSTX. Plasma views with different magnitudes or off axis lines of sight have been easily obtained by changing the relative pinhole-detector distance and their orientation by slightly tilting the instrument.

In order to study the curvature of the X-ray iso-emissivity surfaces and their elongation, the most useful view, with a camera having a limited number of pixels, is one quadrant. In fig. 1, the full reconstruction of the magnetic surfaces carried out by the EFIT code using external magnetic data has been plotted [6,7]; the red frame indicates the full view field of the X-ray camera on a perpendicular plasma cross section (top-out quadrant) with the color contour plot inside. The field of view is about 35 cm x 35 cm, in the intervals $100 < R(cm) < 135$ and $-5 < Z(cm) < 30$, the magnification (defined as the ratio between the distance of detector to pinhole = 10 cm and the distance of pinhole to plasma core ≈ 150 cm), is 1/15 and the projection of each pixel on the cross section of the plasma is 3 cm x 3 cm.

Data have been recorded as counts/pixel at each frame, with an integration time of 1ms (sampling rate 1 kHz), i.e. the same frequency of the EFIT reconstruction (using external coils). The X-ray images presented in this work represent raw data (counts/ms per pixel), without any normalization or correction. In fig 2, three different ways to display the X-ray data are shown, as an example, for one of the shots discussed in the next paragraph: a 3-D plot (counts along the z-axis and x,y being the coordinates of the pixels) in 2a,

contour lines with the same count rate in 2b, and finally, a color contour plot superimposed on the EFIT calculations in 2c. Since in the next paragraph we shall discuss measurements of the plasma elongation, a brief discussion of the errors is required here.

We can identify three different sources of errors:

1) statistical fluctuations due to the sampling
2) optical distortion due to the spatial extension of the detector in the plane perpendicular to the optical axis
3) effect of integration through the plasma of the lines of sight

The counts per pixels per frame (1 ms) range from about 300 for the most external surface up to 2000 for the central peak (see figs. 2a,b). The average number N is therefore of the order of one thousand and the related statistical uncertainty per pixel due to the sampling (shot noise) is $\Delta N/N = 1/\sqrt{N} = 3\ \%$, equivalent to a Signal to Noise Ratio (SNR) per pixel of about 30. Since an iso-emissivity curve is defined by about ten pixels, the statistical uncertainty for its elongation is a factor $\sqrt{10}$ less than for the single pixel. We can therefore claim that the statistical uncertainty for the measurement of the elongation due to the sampling is about 1%.

Due to transverse extent of the detector, the incidence angle of the X-ray photons on the pixel is no longer perpendicular as one moves away from the optical axis. Since the transverse dimension of the detector's active area is very small compared to the focal length, this difference in the incidence angle is of a few degrees only and the resulting optical distortion is very small (less than 2 % over the entire detector). In any case, a pure geometrical corrective factor can be applied to the data to compensate for this effect, if required.

The effect of integration of the lines of sight through the plasma, by far the largest source of uncertainty, is due to geometry and the dependence on the X-ray spectrum. In order to accurately assess these effects, a 3-dimensional code, modeling the spectral X-ray emissivity of the plasma and simulating the image formed on the detector through the pinhole, needs to be developed. We are now interested in estimating the uncertainties, even maximizing them, to show that the experimental results are much higher than even the most exagerated errors. For a given pixel, its line of sight through the plasma maximizes the

contribution of the "tangent" layer ("layer 1"), which the pixel is 'looking at'. We can assess the smearing effect due to the integration through the line of sight, by estimating the spurious contribution of the outer layer ("layer 2"). The optical path in layer 2 is about 25% of that of layer 1. Moreover, we have to consider that emissivity is a peaked function – this, due to the dependence on electron density (Ne), temperature (Te), and impurity concentration (Zeff). We shall consider the 'worst' case: flat Ne and Zeff profiles in the core, as it often occurs in the H-mode. In this case, the only dependence remains that on Te. Since the instrument discriminates the energy of the X-ray photons, the images are obtained by integrating the spectrum from 3 to 8 keV, for a plasma having Te (max) ~ 1 keV. Since in the following analysis we define 2 pixels thick (6 cm) iso-surfaces, we assume that in this radial extention (6 cm), the difference in Te is about 100 eV. This is consistent with the measured temperature profile. Taking into account the spectral distributions with Te=0.8 keV on the "resonant" layer and Te=0.7 keV for the outer one, the "spurious" contribution of the second one is about 40%. Combining therefore the beneficial effects of the tangential view (25%) with the sensitivity to the spectrum (40%) due to the energy discrimination, we conclude that the contribution of outer layer ("2") is roughly 10% of the resonant one ("1"). Further outer layers can be neglected. If we take into account the effect of integration in the vertical plane too, assuming it to be of the same order of magnitude, we got an estimate of 20 % error for the measurement of the elongation. The sensitivity of these images to the spectrum can be exploited to enhance the capability of "tuning" the X-ray energy to the range emitted by a defined region of the plasma, thus minimizing the contribution of the rest of the plasma crossed by the line of sight. As an example of this feature, the ratio between the emissivity of a plasma with Te = 0.6 keV, integrated over the energy spectrum from E to 8 keV, and the emissivity of another layer with all the same parameters but Te = 0.8 keV, is shown in fig. 3, as function of the lower extreme of integration E. Increasing the lower threshold, the contribution of the colder layer with respect to the hotter one can be made smaller and smaller, but with a consequent reduction of the X-ray photon statistics. Therefore, the choice of the energy range is a trade-off between the

intensity of the X-ray signal and the capability of "tuning" on the core plasma, by minimizing the effects of integration along the line of sight.

X-RAY IMAGES AND EFIT CALCULATIONS

As mentioned, the instrument's capability to record X-ray emissions coming from the plasma core has been clearly demonstrated [2]. These images are a good approximation of the plasma cross section since the effects of emissivity integration along the lines of sight are strongly reduced mainly by the sensitivity on the photon spectrum, as discussed in the previous section. In the following a comparison between the measured X-ray surfaces and the calculations of the magnetic surfaces performed by EFIT code, will be discussed, for three shots, having different poloidal beta.

a) # 108727

This is an L-mode shot with additional neutral beam heating (NBI) of 2 MW, plasma current Ip = 0.8 MA, applied toroidal field = 0.55 T and maximum poloidal beta $\beta p = 0.66$.

The superimposition of the color contour-plot of the X-ray images with the EFIT reconstruction shows an excellent agreement for all the times of the discharge, as shown for example in fig.4 at the time t=0.35 s.

b) # 108670

This is an H-mode shot with additional neutral beam heating (NBI) of 5 MW, plasma current Ip = 1 MA, applied toroidal field = 0.44 T . The poloidal beta βp is plotted in fig.5, and it reaches a value of 0.72. The EFIT code reconstructs a positive shear and an elongation on axis of 1.5, which is constant during the current flat-top. Also in this case the agreement between the X-ray images and EFIT calculations is excellent at all the times. In fig.6 a comparison in shown at the time t = 0.35s, when $\beta p = 0.6$.

b) # 108729

This is an H-mode shot with additional neutral beam heating (NBI) of 5 MW, plasma current Ip = 0.8 MA, toroidal field = 0.49 T . The poloidal beta βp is plotted in fig.7; it increases in time, being below 0.6 up to t = 0.25 s and reaching the record value of 1.2 at t = 0.35 s. In fig. 8, X-ray images and magnetic surfaces are shown for 4 different times. At the beginning of the

plateau (fig. 8a) when βp is less than 0.6 the agreement is very good, like in the previously discussed shots. But at later times, the disagreement becomes more and more evident as βp approaches the value 1.2. The figures 8 b,c,d, show indeed that the X-ray emissivity surfaces are evolving toward a circular shape, while, in contrast, EFIT reconstructs a progressive increase of the elongation for magnetic flux surfaces. In order to assess quantitatively the elongation of the X-ray surfaces, we identified three curves with same counts in the contour plot, labeled 2 (outer), 1(middle) and 0 (inner). In fig 9 the color contour plot is shown (t = 0.3 s) as function of the pixel position together with the color code for counts/ms. Since these are curves at constant counts, they move outward at later times due to the increase of the X-ray plasma emissivity. In fig.10 the measured elongation of these three X-ray surfaces E(2), E(1), E(0) is plotted vs time and compared with the elongation on axis E(0) predicted by the EFIT code. Error bars (20%), estimated in the previous paragraph, are shown just for the curve E(1). It is evident that both the variations of elongation and the discrepancies with respect to the EFIT calculations are well beyond the experimental uncertainties. EFIT reconstructs also a reversed shear starting at 230 ms, as indicated in fig.10, together with an increase in the central value of the safety factor q0.

It is therefore clear than, for shots at high poloidal beta (1.2), the EFIT reconstruction of the magnetic surfaces does not match with the X-ray iso-emissivity surfaces. No instrumental effects can be invoked to explain this difference. The X-ray camera has the same view, configuration and acquisition parameters for these three shots. The shots 108670 and 108729 are both in the H-mode, with the same power input (5 MW NBI) and consequently comparable levels of X-ray emissivity. As final confirmation of the reliability of the measurements there is the agreement up to t = 0. 25 s even in the shot 108729, when βp is less or equal to 0.6, like in the shot 108670.

This difference can be due to several sources including:

i) the lack of internal magnetics measurements

ii) the assumption of zero toroidal rotation

iii) X-ray emission that is not aligned with magnetics surfaces

In order to explain the observed difference, simulations of the X-ray emissions, taking into account the 3-D maps for Ne, Te and Zeff, will be required to derive the pressure surfaces and then make comparisons with the magnetic reconstructions that include plasma rotation effects. Indeed the centrifugal effect due to the toroidal rotation can change the density profile, producing a less elongated pressure profile. Once the model is evaluated, these X-ray images could be used to constrain the reconstructions. It also reflects on the powerful capabilities of this instrument to investigate the plasma core in 2-D and with good time resolution, with high contrast and accuracy, even with a limited number of pixels.

CONCLUSIONS

The X-ray images of the NSTX plasma core, obtained with this innovative device mounted on NSTX with a tangential view of the plasma, allowed the measurement of the elongation of the X-ray iso-emissivity contour. Comparison with EFIT calculations revealed that the agreement is excellent for shots with low or moderate poloidal beta (0.6). At high poloidal beta (1.2) the code predicts an increase of the elongation of the magnetic surfaces from 1.5 to 2.2, while the X-ray images show iso-emissivity surfaces becoming circular.

Such comparisons are possible due to the low noise and high contrast imaging capability of this instrument, working in photon counting mode with energy discrimination, at very high X-ray fluxes. This diagnostic allows therefore the investigation of the plasma core in all the configurations, with good time resolution ($\leq$ 1 ms), even in ohmic cases, with very low levels of X-ray emissivity and in very clean plasmas, like those obtained in NSTX. Instruments based on the more traditional technique of visible conversion of the X-ray photons, imaging intensifier and CCD detector cannot be routinely used as plasma diagnostic, due to their intrinsic lower efficiency and signal to noise vales. This is indeed confirmed by the experience obtained in the PBX-M experiment, where an X-ray tangential camera based on phosphor conversion and intensified CCD camera [8] worked successfully, but for very

limited plasma scenarios, with high radiated power and Zeff values, and without a good time resolution.

As operated presently, the efficiency of the instrument was limited only by the thick beryllium window (400 μm) on the machine; its replacement with a 12 μm one, will increase the efficiency by an order of magnitude, allowing the use of this diagnostic even with plasmas having much lower X-ray emissivities.

These results show that it will be possible, with such a device, to derive the shape of the pressure surfaces, providing a further constraint for the reconstruction of the internal magnetic surfaces and of such an important plasma parameter as the safety factor profile.

Acknowledgements:

The laboratory experiments performed at the Johns Hopkins University have been supported by US DOE Grant DE-FG02-86ER53214.

REFERENCES

[1] D. Pacella et al., Rev. Sci. Intrum. Vol 72, N° 2 (2001)

[2] D. Pacella et al., Rev. Sci. Intrum. Vol 74, N° 3 (2003)

[3] R. Bellazzini et. al., Nuclear Instruments and Method Phys. Res. A 419, (1998) 429

[4] R. Bellazzini et. al., Nuclear Instruments and Methods Section A471 (2001) 41

[5] M. Ono et al., Nucl Fusion 40 (2000) 557

[6] S. A. Sabbagh et al., Nucl. Fusion 41, (2001) 1197

[7] L.Lao et al., Nucl. Fusion 25 (1985) 1611

[8] E. T. Powell et al., Nucl. Fusion 33 (1993) 1493

FIGURE CAPTIONS

1) Reconstruction of the magnetic surfaces carried out by the EFIT code : the yellow frame indicates the full view field of the X-ray camera on a perpendicular plasma cross section (top-out quadrant) with the color contour plot inside. The view field is about 35 cm x 35 cm, in the intervals $100 < R(cm) < 135$ and $-5 < Z(cm) < 30$

2) X-ray data display: 2a) 3-D plot of intensity (counts/ms) in z-axis and coordinates of the pixels in x,y ; 2b) contour lines of intensity (counts/ms); 2c) color contour plot of intensity superimposed on EFIT calculations.

3) Ratio between the emissivity of a plasma with Te = 0.6 keV, integrated over the energy spectrum from E to 8 keV, and the emissivity of another layer with all the same parameters but Te = 0.8 keV, as function of the lower extreme of integration E.

4) Shot # 108727, with Ip = 0.8 MA, applied toroidal field = 0.55 T and maximum poloidal beta $\beta p = 0.66$ Superimposition of the color contour-plot of the X-ray images with the EFIT reconstruction at time t=0.35 s

5) Poloidal beta βp for shot # 108670

6) Shot # 108670 with Ip = 1 MA, applied toroidal field = 0.44 T and maximum poloidal beta $\beta p = 0.72$. Superimposition of the color contour-plot of the X-ray images with the EFIT reconstruction at time t=0.35 s

7) Poloidal beta βp for shot # 108729

8) Shot # 108729 with Ip = 0.8 MA, applied toroidal field = 0.49 T and maximum poloidal beta $\beta p = 1.2$. Superimposition of the color contour-plot of the X-ray images with the EFIT reconstruction at time t=0.23 s (a) , t=0.31 s (b), t=0.4 (c), t=0.5 s (d).

9) Color contour plot for # 108729 (t = 0.3 s) as function of the pixel position, where the three iso-emisivity curves 2,1,0 have been identified

10) Shot # 108729. Measured elongations of these three X-ray surfaces E(2), E(1), E(0) plotted vs time and compared with the elongation on axis E(0)EFIT predicted by the EFIT code. Error bars (20%) are shown just for the curve E(1)

FIGURES

Fig. 1

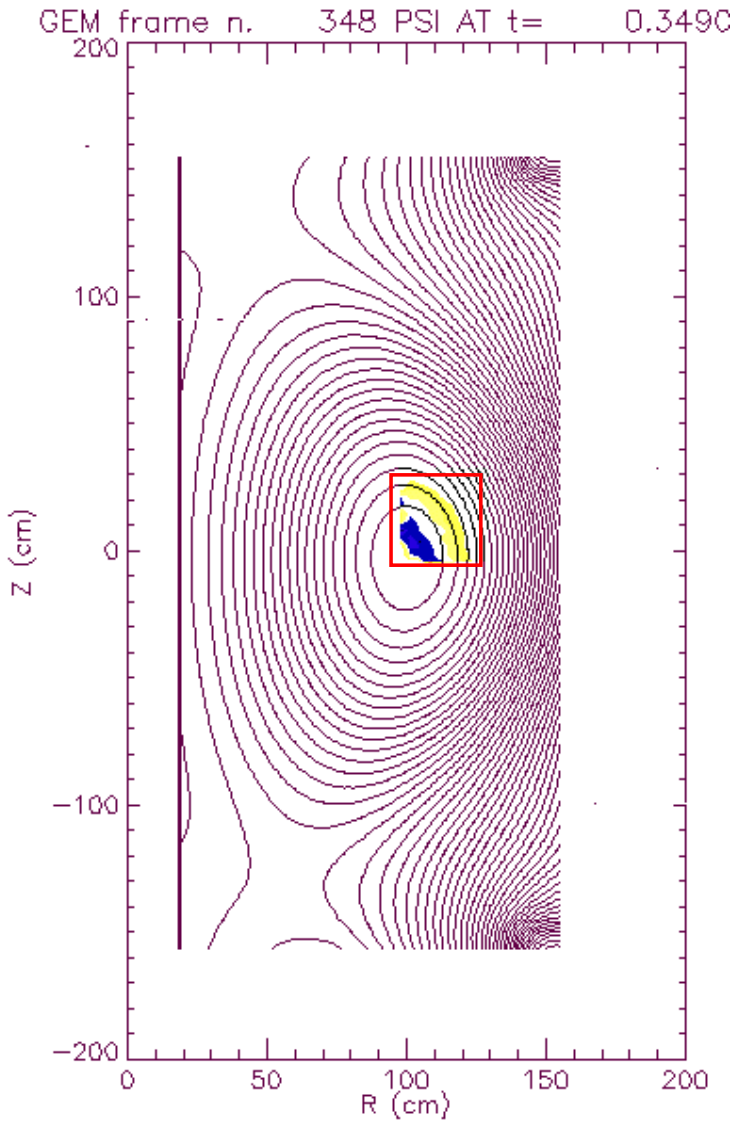

2 a

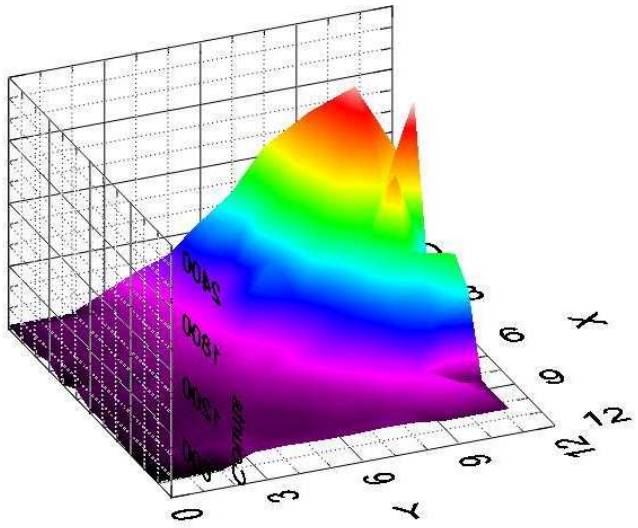

2 b

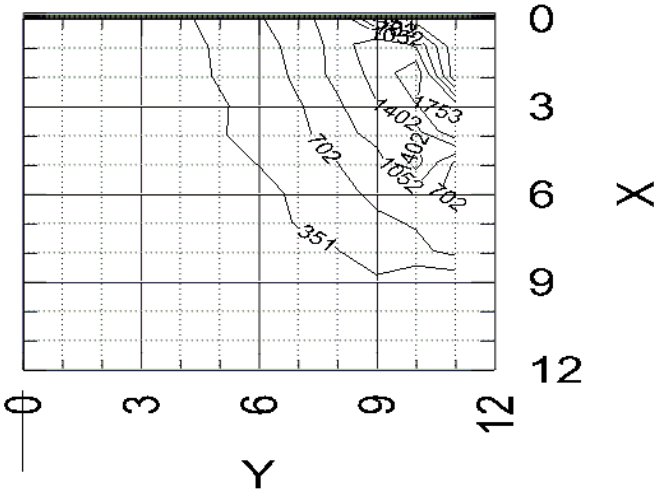

2 c

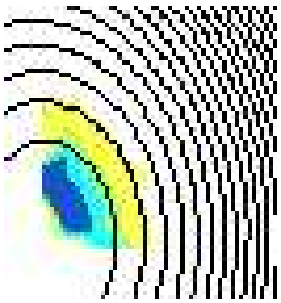

Fig. 3

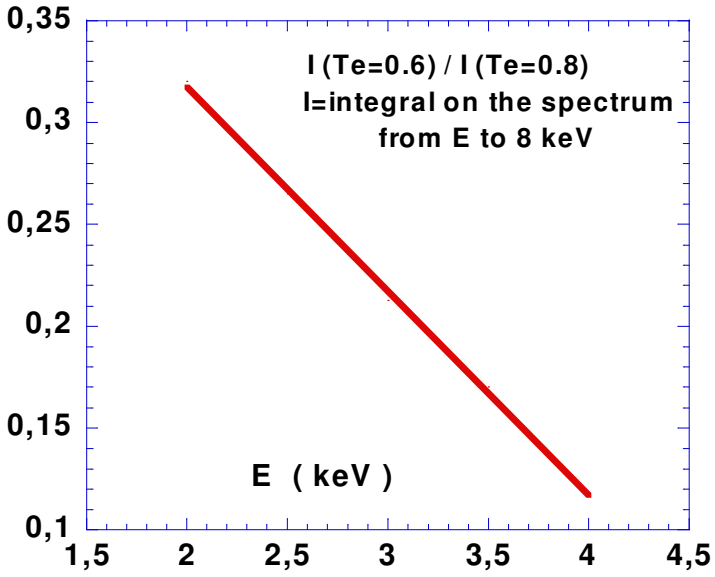
I (Te=0.6) / I (Te=0.8)
I=integral on the spectrum
from E to 8 keV
E (keV)
0,35
0,3
0,25
0,2
0,15
0,1
1,5
2
2,5
3
3,5
4
4,5

Fig. 4 **t = 0.35 s** #108727

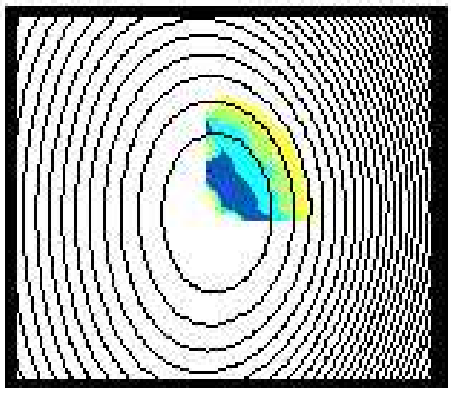

Fig. 5

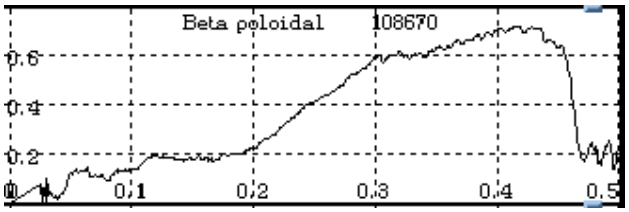

Fig 6 **#108670** t = 0.35 s

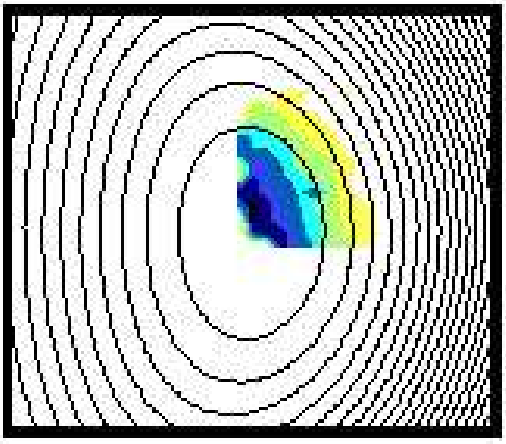

Fig. 7

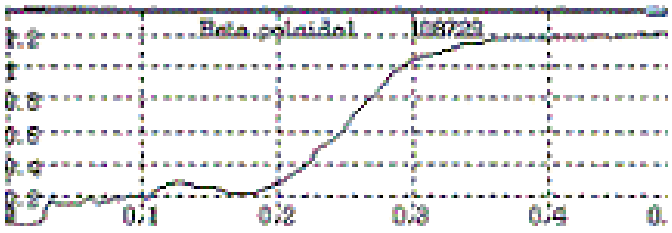

Fig 8

a t= 0.23 s **b t = 0. 31 s**

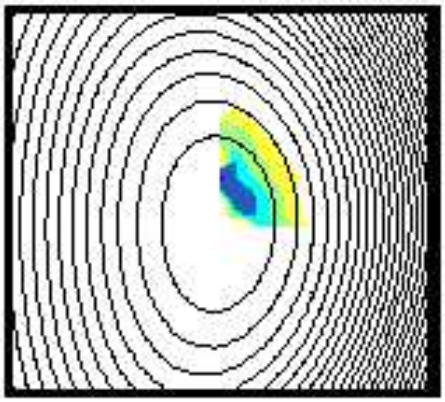

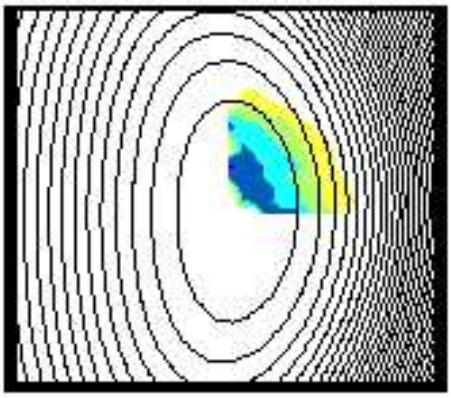

c t = 0.4 **d t=0.5**

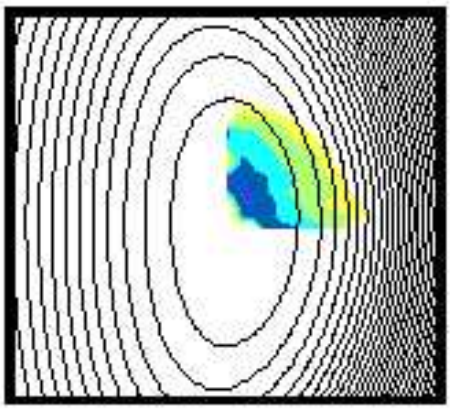

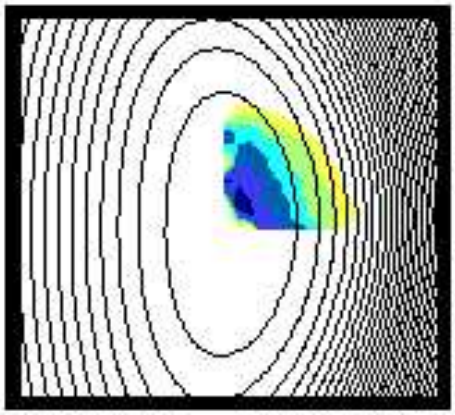

Fig. 9

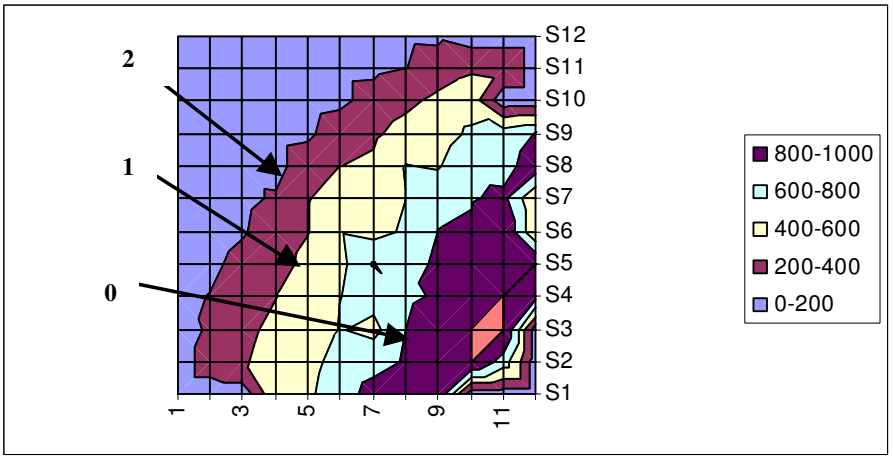

Fig. 10

Elongation

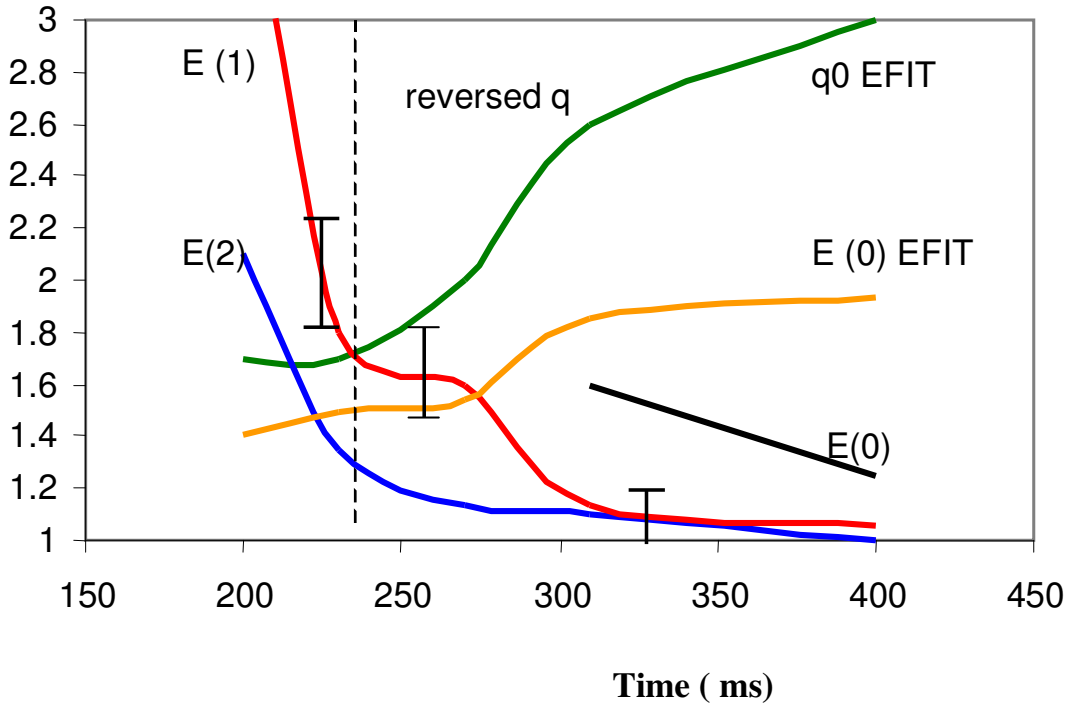

External Distribution

Plasma Research Laboratory, Australian National University, Australia

Professor I.R. Jones, Flinders University, Australia

Professor João Canalle, Instituto de Fisica DEQ/IF - UERJ, Brazil

Mr. Gerson O. Ludwig, Instituto Nacional de Pesquisas, Brazil

Dr. P.H. Sakanaka, Instituto Fisica, Brazil

The Librarian, Culham Laboratory, England

Mrs. S.A. Hutchinson, JET Library, England

Professor M.N. Bussac, Ecole Polytechnique, France

Librarian, Max-Planck-Institut für Plasmaphysik, Germany

Jolan Moldvai, Reports Library, Hungarian Academy of Sciences, Central Research Institute for Physics, Hungary

Dr. P. Kaw, Institute for Plasma Research, India

Ms. P.J. Pathak, Librarian, Institute for Plasma Research, India

Ms. Clelia De Palo, Associazione EURATOM-ENEA, Italy

Dr. G. Grosso, Instituto di Fisica del Plasma, Italy

Librarian, Naka Fusion Research Establishment, JAERI, Japan

Library, Laboratory for Complex Energy Processes, Institute for Advanced Study, Kyoto University, Japan

Research Information Center, National Institute for Fusion Science, Japan

Dr. O. Mitarai, Kyushu Tokai University, Japan

Dr. Jiangang Li, Institute of Plasma Physics, Chinese Academy of Sciences, People's Republic of China

Professor Yuping Huo, School of Physical Science and Technology, People's Republic of China

Library, Academia Sinica, Institute of Plasma Physics, People's Republic of China

Librarian, Institute of Physics, Chinese Academy of Sciences, People's Republic of China

Dr. S. Mirnov, TRINITI, Troitsk, Russian Federation, Russia

Dr. V.S. Strelkov, Kurchatov Institute, Russian Federation, Russia

Professor Peter Lukac, Katedra Fyziky Plazmy MFF UK, Mlynska dolina F-2, Komenskeho Univerzita, SK-842 15 Bratislava, Slovakia

Dr. G.S. Lee, Korea Basic Science Institute, South Korea

Institute for Plasma Research, University of Maryland, USA

Librarian, Fusion Energy Division, Oak Ridge National Laboratory, USA

Librarian, Institute of Fusion Studies, University of Texas, USA

Librarian, Magnetic Fusion Program, Lawrence Livermore National Laboratory, USA

Library, General Atomics, USA

Plasma Physics Group, Fusion Energy Research Program, University of California at San Diego, USA

Plasma Physics Library, Columbia University, USA

Alkesh Punjabi, Center for Fusion Research and Training, Hampton University, USA

Dr. W.M. Stacey, Fusion Research Center, Georgia Institute of Technology, USA

Dr. John Willis, U.S. Department of Energy, Office of Fusion Energy Sciences, USA

Mr. Paul H. Wright, Indianapolis, Indiana, USA

The Princeton Plasma Physics Laboratory is operated
by Princeton University under contract
with the U.S. Department of Energy.

Information Services
Princeton Plasma Physics Laboratory
P.O. Box 451
Princeton, NJ 08543

Phone: 609-243-2750
Fax: 609-243-2751
e-mail: pppl_info@pppl.gov
Internet Address: http://www.pppl.gov